Tutor/s

Dra. Amparo Caubet Marin
Departament de Química Inorgànica i Orgànica, Secció de Química Inorgànica

Grau de Química

Treball Final de Grau

Synthesis of ruthenium (II) compounds with 2,2': 6',2''-terpyridine derived ligands.

Síntesis de compostos de ruteni(II) amb lligands derivats de 2,2': 6',2''-terpiridina.

Laura Pérez Relaño

June 2021

Universitat de Barcelona

B:KC Barcelona Knowledge Campus
Campus d'Excel·lència Internacional

“Progress depends on our brain. The most important part of our brain, that which is neocortical, must be used to help others and not just to make discoveries.”

Rita Levi-Montalcini

Voldria agrair a la Dra. Amparo Caubet Marin per tot el compromís i temps dedicat en orientar-me durant aquest projecte, sense perdre els ànims quan les coses no sortien de la manera esperada.

A la resta de professors que han participat i, per descomptat, als meus companys de laboratori per tota l’ajuda i el bon ambient. També a les meves amigues de la universitat per recolzar-nos i compartir els moments de preocupació.

A totes les persones properes que m’han escoltat i han posat el seu gra de sorra, en especial, a la Marta i el Ben per llegir-se amb interès el treball.

Per acabar, agrair a la meva família la seva paciència i ànims incondicionals.

REPORT

CONTENTS

1. SUMMARY

Three new ligands ((4'-(4-bromophenyl)-2,2':6',2''-terpyridine (**4a**), 4'-(4-aniline)-2,2':6',2''-terpyridine (**4b**), 4'-(2-aminopyridine-3-yl)-2,2':6',2''-terpyridine (**4c**)) have been prepared by combination of Kröhnke condensation and Michael addition. Compound **4a** reacts with $RuCl_3 \cdot 3H_2O$ in methanol producing [Ru(Brterpy)Cl_3] (**5a**). The reaction of **5a** with bidentate ligands, namely 2,2'-bipyridine and 1,10-phenanthroline, allows to obtain two monofunctional ruthenium (II) compounds: [Ru(Bipy)(Brterpy)Cl]Cl (**7a**) and [Ru(Brterpy)Cl(Phen)]Cl (**7a'**), respectively.

The ligands and the ruthenium (II) complexes were characterized by infrared spectroscopy (IR) and mono- and bidimensional NMR spectroscopies. The metal compounds were also characterized by mass spectrometry. Furthermore, the study of the absorbance by UV-Vis and their fluorescence by the emission and excitation spectra were carried out.

Finally, DNA interaction with complexes **7a** and **7a'** was studied contrasting the effect with non-irradiated and irradiated samples with photoactivating wavelength light. The evidence from this study suggests that both complexes can act has photosensitizers.

Keywords: Ruthenium complexes, 2,2':6',2''-terpyridine ligands, antitumoral metal-based drugs, photosensitizers, photodynamic therapy.

2. RESUM

Tres nous lligands ((4'-(4-bromofenil)-2,2':6',2''-terpiridina (**4a**), 4'-(4-anilina)-2,2':6',2''-terpiridina (**4b**), 4'-(2-aminopridina-3-il)-2,2':6',2''-terpiridina (**4c**)) han estat preparats a partir de la combinació de la condensació de Kröhnke i l'addició de Michael. El compost **4a** reacciona amb el $RuCl_3 \cdot 3H_2O$ en metanol obtenint-se [Ru(Brterpy)Cl_3]. La reacció de **5a** amb els lligands bidentats, 2,2'-bipiridina i 1,10-fenantrolina, permet obtenir dos compostos de ruteni (II) monofuncionals: [Ru(Bipy)(Brterpy)Cl]Cl (**7a**) i [Ru(Brterpy)Cl(Phen)]Cl (**7a'**), respectivament.

Aquests lligands i els complexes de ruteni (II) han estat caracteritzats per espectroscòpia d'infraroig i espectroscòpies mono- i bi-dimensional de RMN. Els compostos metàl·lics també han estat caracteritzats per espectrometria de masses. A més a més, l'estudi de la seva absorbància pel UV-Vis i la seva fluorescència a partir dels espectres d'emissió i excitació duts a terme.

Per acabar, s'ha estudiat la interacció dels complexes (**7a**,**7a'**) amb el ADN comparant l'efecte de mostres irradiades i no irradiades amb la longitud d'ona adient per activar-los. Les evidències d'aquests estudies suggereixen que els dos complexes poden actuar com a fotosensibilitzadors.

Paraules clau: Complexes de ruteni, lligands 2,2':6',2''-terpiridina, fàrmacs antitumorals basats en metalls, fotosensibilitzadors, teràpia fotodinàmica.

3. INTRODUCTION

Metal-based drugs and imaging agents are extensively used in the clinic for the treatment and diagnosis of cancer and wide range of other diseases. One of the most interesting transition metal complexes used for cancer treatments is cisplatin (*cis*-diamminedichloridoplatinum(II)) (Scheme 1) that was synthetized in the 1845 by Michele Peyrone [1]. Later, Barnett Rosenberg (1965) discovered some of its important properties as the inhibition of division in Escherichia Coli cells and its antitumor activity [2,3] and in 1978 it was approved by the US Food and Drug Administration (FDA) for testicular and ovarian cancer. However, its use is limited by the severe side effects that it presents like neurotoxicity and nephrotoxicity, its low solubility, and the appearance of resistance [4,5]. This encouraged the investigation on complexes cisplatin analogues to develop new drugs with improved efficiency and reduced side effects. Nowadays, besides cisplatin, carboplatin (*cis*-diammine-(1,1-cyclobutane dicarboxylato)platinum(II)) and oxaliplatin (*1R,2R*-diaminocyclohexaneoxalatoplatinum(II)) (Scheme 1) are used in clinical therapy for different types of tumors with much success [6,7], but they do not show substantial advantages over cisplatin [8].

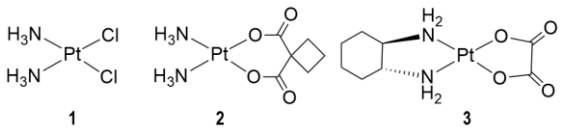

Scheme 1. Structures of cisplatin (1), carboplatin (2) and oxaliplatin (3).

The target for these antitumor compounds is genomic DNA. They can bind efficiently to the N-7 atoms of the purine bases and form the adducts 1,2-intrastrand d(GpG) and d(ApG) cross-linked. This induces a conformational change in its structure blocking the transcription and replication of the DNA [9].

Due to the limitations of the currently approved platinum drugs against cancer, the development of new classes of compounds it is needed. Many other metal complexes have been shown to possess bioactivity and several drugs based on them have been developed [10,11]. Within this field, there is increasing attention on the use of Ru (II) complexes [12]. There are three main properties that make ruthenium complexes well suited for medical applications: (i) the rate of

ligand exchange, (ii) the range of accessible oxidation states and (iii) the ability of ruthenium to mimic iron and bind to certain biological molecules. Furthermore, ruthenium tends to form octahedral complexes, which gives the opportunity to have two more ligands to expand the possibilities of its structures. This feature gives an advantage over platinum (II) complexes, which adopt a square planar geometry with less achievable structures. Ruthenium can also form strong chemical bonds with a range of different elements of diverse chemical "hardness" and electronegativities, meaning that it can bind to a range of biomolecules, not just DNA.

Two ruthenium derivatives, imidazolium *trans*-tetrachloridedimetilsulfoxideimidazole ruthenate(III) (NAMI-A) and imidazolium *trans*-tetrachloridobis(1H-indazole)ruthenate(III)] (KP-1019) (Scheme 2, 5 and 4) have shown positive out-comes after phase II clinical trials, showing the ability both to prevent the formation of metastases and to inhibit their growth [13]. On the other hand, among the ruthenium(II) organometallic complexes, the half sandwich arene-ruthenium subgroup, is particularly promising in the field of cancer therapy. Two compounds [Ru(p-cymene)Cl(en)] (READ-C) and [Ru(p-cymene)Cl_2(pta)], where pta= 1,3,5-tri-aza-7-phosphaadamantane (RAPTA-C) (Scheme 2, 6 and 7, respectively) have shown relevant therapeutic potential [14].

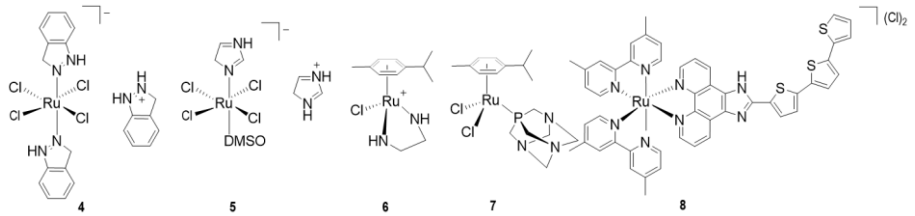

Scheme 2. Structures of KP1019 (4), NAMI-A (5), READ-C (6) and RAPTA-C (7) TLD-1433 (8).

Some of these complexes can form covalent bonds with guanine bases of DNA affecting replication and transcription leading to cell death as cisplatin. The biological target of another group of complexes is metal-transporting blood proteins such as albumin and transferrin. Also, ruthenium(II) complexes with arene ligands are inhibitors of protein kinase that have vital roles in cell biology. In general, impacting the mitochondrial pathway and ROS mediated apoptosis are the principal mechanisms of action of ruthenium(II) compounds. Additionally, light irradiation of these compounds was shown to enable DNA cleavage, highlighting their potential use as photosensitizers (PSs) for photodynamic therapy (PDT) (Scheme 3) [15]

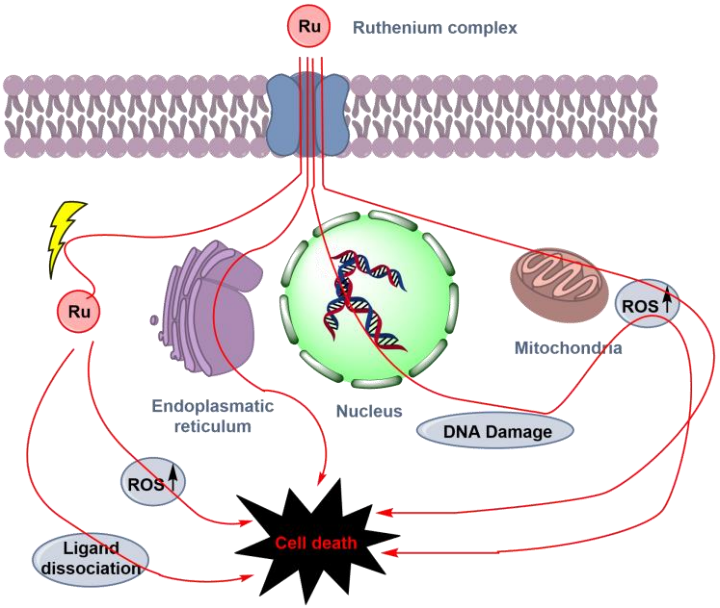

Scheme 3. General targets of ruthenium complexes.

Photodynamic therapy is a medical technique which consists of the light activation of a photosensitizer [16]. Some Ru (II) compounds can act as photosensitizers (PS) when they are light irradiated at their wavelength in the range of absorption, causing a metal-to-ligand (MLCT) energy transfer [17]. The PS reaches a singlet excited state (^{1}MLCT) and undergoes intersystem crossing, so the excited state becomes a triplet character (^{3}MLCT).

At this stage, two mechanisms are possible (Scheme 4). The Type I will undergo an electron or proton exchange from the PS triplet excited state to biological substrates. This process produces ROS as superoxide, hydroxyl radicals or peroxides, and leads to apoptosis with low cytotoxicity. Type II transfers the triplet excited state energy to molecular oxygen which is very reactive with the surrounding biomolecules and generates cellular damage. This second mechanism is the most common in therapies nowadays.

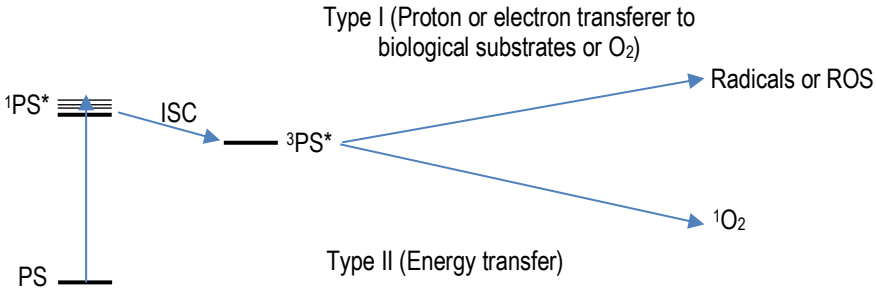

Scheme 4. Mechanisms of action of Photodynamic therapy.

Nonetheless, solid tumors have low levels of oxygen and this is a big limitation for PDT efficacy. Photoactivated chemotherapy is another option that is independent of oxygen levels and has two possible mechanisms. In the first, ruthenium photoactivated complexes dissociate from the ligand and targets DNA. In the seconds, light activates the complexes and releases a bioactive compound which leads to cell death.

Ruthenium(II) polypyridyl complexes are receiving increasing attention due to their promising anticancer and antimicrobial activity as chemotherapeutic agents as well as photodynamic therapy (PDT) photosensitizers (PSs) [18-20]. One of these ruthenium-based PDT PSs, namely TLD-1433 (Scheme 2, 8), just completed a phase I clinical trial as a PDT PS against bladder cancer [21].

Furthermore, the 2,2';6',2''-terpyridine (tpy) derivatives are also chelating ligands suitable for the formation of transition metal complexes [22]. These complexes have photodynamic behavior so they can be activated with light. Also, their ability to bind and cleave DNA has been observed. In cancer therapies, the specificity of the drugs is crucial. The functionalized terpyridine derived ligands are bioconjugable with protein vectors [23]. These proteins can recognize specific membrane receptors overexpressed on the surface of the damaged cells. This ability gives the opportunity to transport the design complex to the tumor cells.

4. OBJECTIVES

The aim of this project is the preparation and characterization of ruthenium compounds with 2,2':6',2''-terpyridine ligands with different functional groups at 4'-position and study their interaction with DNA. This objective can be broken down as follows:

- The synthesis and characterization of new 2,2':6',2''-terpyridine derived ligands.
- The synthesis and characterization of the ruthenium complexes with these ligands.
- Study of their absorption, emission, and excitation spectra and the interaction with DNA by electrophoresis.

5. RESULTS AND DISCUSSION

5.1. SYNTHESIS AND CHARACTERIZATION OF LIGANDS

The general method used for the synthesis of 4'-functionalizated 2,2':6',2''-terpyridine ligands is shown in Scheme 5 [24].

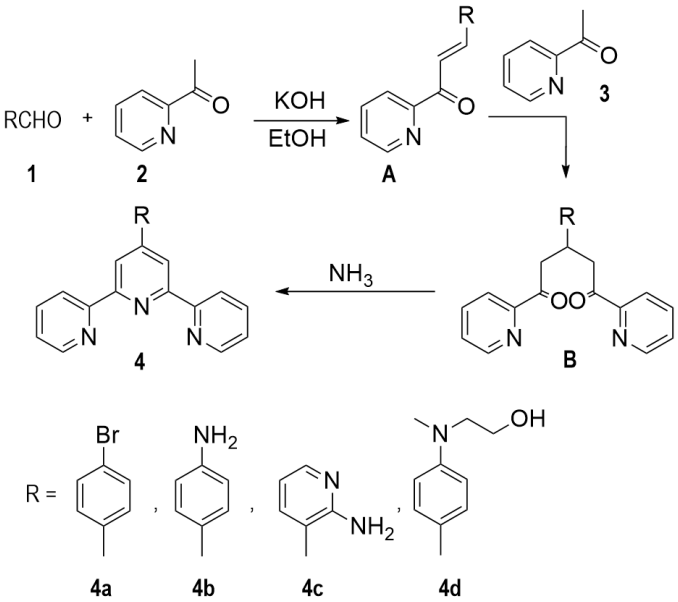

Scheme 5. Synthesis of ligands.

The first step of this reaction is a Kröhnke condensation of 2-acetylpyridine (**2**) with the aldehydes (**1a, 1b, 1c, 1d**) to form the enone (chalcone) (**A**). The next step is a Michael addition of a second molecule of 2-acetylpyridine forming the 1,5-dione (**B**). The final reaction is the cyclization with ammonium as a nitrogen source to form the central pyridine ring closure completing the terpyridine ligand.

The 4'-(4-bromophenyl)-2,2':6',2''-terpyridine (Brterpy;**4a**), 4'-(4-aniline)-2,2':6',2''-terpyridine (Anilineterpy;**4b**) 4'-(2-aminopyridine-3-yl)-2,2':6',2''-terpyridine (Aminopy;**4c**) were successfully obtained by this method while it wasn't possible to synthesize 4'-(*N*-(2-hydroxyethyl)-*N*-methyl)-2,2':6',2''-terpyridine (**4d**).

In the case of ligand **4c** the crude product was an oil that needed to be to passed through a SiO_2 column using ethyl acetate:hexane (1:4) as eluent to purify (see Experimental section). The final yield was so low that only characterization was possible.

The ligand 4'-((naphthalen-2-yl)methoxy)-2,2':6',2''-terpyridine (**4e**) was prepared as previously reported [25] using the reaction of nucleophilic replacement of 4'-chloro-2,2':6',2''-terpyridine with 2-naphthalenemetha-nol in dry DMSO in the presence of base (KOH) (see Scheme 6 below).

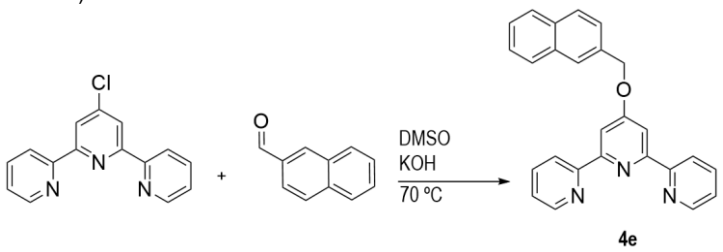

Scheme 6. Synthesis of ligand 4'-((naphthalen-2-yl)methoxy)-2,2':6',2''-terpyridine (**4e**).

The ligands were characterized by IR and mono- and two-dimensional (^1H,^{13}C {^1H } and HSQC) NMR spectroscopies (see Experimental section). The solid-state IR spectra of new ligands show the typical bands of the terpyridine compound, with the most characteristic being a strong band in the region 1580−1616 cm^{-1} assigned to ν(C=N) stretching.

All these ligands show a similar ^1H-NMR spectrum. The characteristic signal is the singlet which appears in the range 8.5-9.0 ppm and indicates that the 4'-substituted-2,2':6',2''-terpyridine ligand has been formed. In the spectrum of ligand **4e** a singlet can be seen at 5.50 ppm due to the methylene group.

In the case of the 4'-(*N*-(2-hydroxyethyl)-*N*-methyl)-2,2':6',2''-terpyridine (**4d**) since the general method did not work, preparation was tried following the process described in [26]. The procedure is essentially the same reactions but using solventless conditions involving sequential aldol and Michael addition reactions.

The oil obtained was purified by chromatography SiO_2 column. The only isolated products were the starting aldehyde **1d** and the alcohol produced in its reduction (see Appendix).

5.2. SYNTHESIS AND CHARACTERIZATION OF RUTHENIUM (II) COMPLEXES

The $[RuCl_2(dmso)_4]$ compound was synthesized to use as a precursor of ruthenium (II) complexes (Scheme 7) [27].

$$RuCl_3 \cdot 3H_2O \xrightarrow[\Delta]{DMSO} RuCl_2(DMSO)_4$$

Scheme 7. Synthesis of dichloridotetrakis(dimethylsulfoxide)ruthenium(II).

The reaction for the synthesis of dichloridotetrakis(dimethylsulfoxide)ruthenium(II) is a reduction-oxidation which needs an intense reflux with elevated temperature and vigorous stirring. It is characterized by IR showing the Csp^3-H stretching bands at 3000 cm^{-1} of the methyl groups and by ^1H NMR. The ^1H spectrum shows different signals due to the methyl groups of DMSO coordinated [28], which can have three S-bonded Me_2SO molecules for each O-bonded.

When this compound was used as a starting material in the reaction with terpyridine derived ligands, a mixture of isomers were obtained that were difficult to separated (Scheme 8).

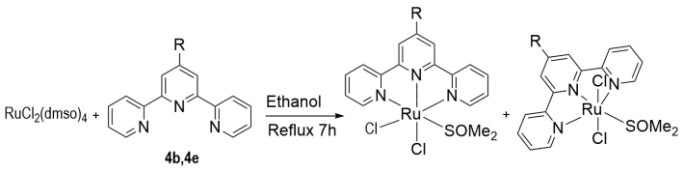

Scheme 8. Synthesis ruthenium(II) complexes.

The use of $RuCl_3 \cdot 3H_2O$ as a precursor has given better results. It has the advantage of avoiding formation of geometric isomers (Scheme 9) [29].

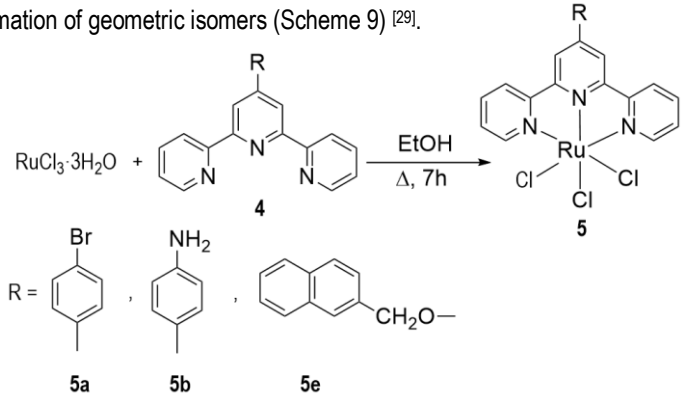

Scheme 9. Synthesis of ruthenium (III) complexes, $[Ru(Rterpy)Cl_3]$.

Due to their low solubility and paramagnetic properties, the three ruthenium (III) compounds obtained have been characterized by elemental analysis and IR spectra. Elemental analysis confirmed the pure obtention of [Ru(Brterpy)Cl_3] (**5a**) compound. The analytical results of [Ru(Anilineterpy)Cl_3] (**5b**) and [Ru(Nterpy)Cl_3] (**5e**) are too low, probably suggesting that some $RuCl_3$ remains unreacted due its low insolubility and because the reaction time was not enough.

With the aim to obtain Ru (II) compounds, type [Ru(Rterpy)(Nterpy)]$^{2+}$, the [Ru(Nterpy)Cl_3] was reacted with **4a** and **4b** which have one reactive group (R = Br or Aniline) that can modulate their properties. The method [30] consists of a redox reaction with N-ethylmorpholine a reducing agent in a methanolic solution under a N_2 atmosphere. The product was precipitated as a PF_6 salt (Scheme 10).

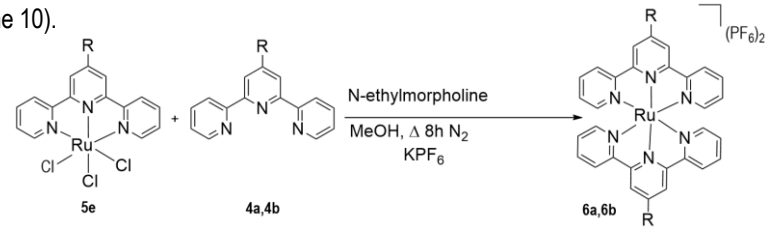

Scheme 10. Synthesis of [Ru(Nterpy)(Rterpy)]$(PF_6)_2$

The two solids obtained (red **6a**, brown **6b**) were characterized by MS and ^{1}H NMR, in both cases a mixture of products is observed. The cause could be having started from the product **5e** that later was found out that was contaminated.

Another type of ruthenium(II) complexes was synthesized, [RuCl(N,N')(Rterpy)]Cl, where R= Br or aniline and N,N'= bidentate ligands (Scheme 11). These kinds of monofunctional compounds could be interesting for their attractive photophysical properties that in general are present in ruthenium polypyridyl complexes [20,30,31]. In addition, these compounds could have the ability to intercalate and coordinate the DNA because they can release their labile ligand forming the aqua species. This aqua species could bind to the DNA nucleobase, in a similar way to cisplatin.

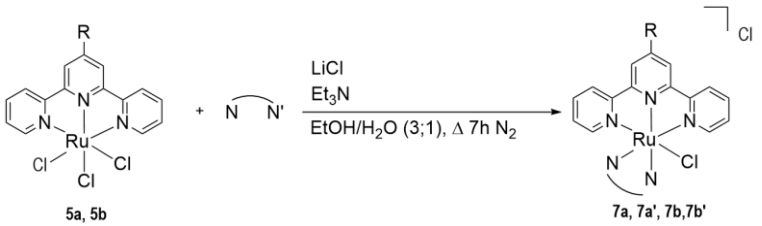

Scheme 11. Synthesis of monofunctional complexes [RuCl(N,N')(Rterpy)]Cl.

The reaction of [Ru(Brterpy)Cl_3] (**5a**) with an equimolar amount of ligands 2,2'-bipyridine or 1,10-phenantroline using triethylamine as reducing agent and excess of LiCl under N_2 atmosphere [32] produced a dark solid in both cases. Its characterization data (see Experimental Section and Appendix) agreed with the expected structures for [Ru(Bipy)(Brterpy)Cl]Cl (**7a**) and [Ru(Brterpy)Cl(Phen)]Cl (**7a'**).

The ^{1}H-NMR spectra of **7a** and **7a'** are consistent with the symmetric Brterpy in the equatorial plane with the bidentate ligands (Bipy or Phen) perpendicular so the two halves of the (N,N') ligand are not equivalents. The ^{1}H peaks of the halves over the tpy plane are closer to the axial chloride therefore they are shifted downfield compared to the corresponding proton on the other ring. For instance, the [Ru(Brterpy)Cl(Phen)]Cl δ_{H^a} = 10.45 ppm vs. $\delta_{H^{a'}}$ = 7,71 ppm (Scheme 12). The protons of the terminal aromatic rings of the tpy ligand are also affected by the coordination when compared with the free ligand while the singlet corresponding to the H^7 of the terpyridine keeps appearing at 8.5-9.0 ppm. Also, these complexes were characterized by spectroscopic mass showing the molecular pics at 682 m/z (**7a**) and 706 m/z (**7a'**).

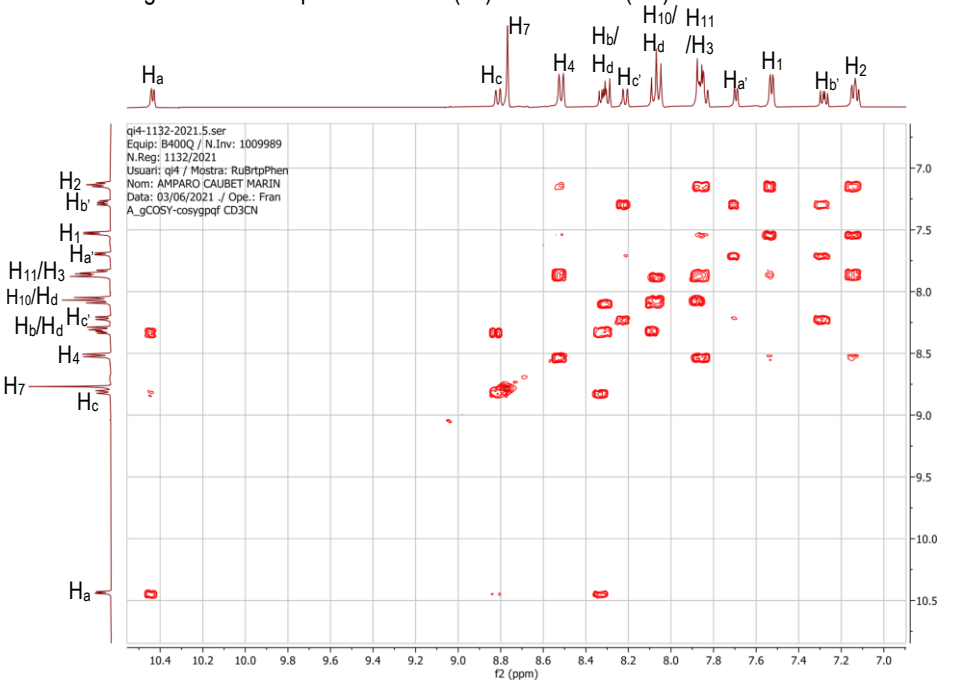

Scheme 12. Bidimensional NMR {^{1}H, ^{1}H}-COSY spectrum of **7a'** in acetonitrile-d_3.

When the starting reactive is [Ru(Anilineterpy)Cl_3] (**5b**) the products obtained are [Ru(Anilineterpy)(Bipy)Cl]Cl (**7b**) impurified with tris(2,2'-bipyridyl)ruthenium(II) and [Ru(Anilineterpy)Cl(Phen)]Cl (**7b'**) mixed with tris(1,10-phenantroline)ruthenium(II).

5.2.1. UV-VIS STUDIES OF THE RUTHENIUM(II) COMPLEXES

The UV-Vis spectra of the two complexes **7a** and **7a'** show the maximum wavelength absorption and the absorptivity (ε) used for the further fluorescence studies.

$$A = \varepsilon\, c\, l$$

Equation 1. Lamber-Beer law.

Entrada	Absorbance ($\lambda_{màx}$)	ε (l mol^{-1} cm^{-1})
7aa	490 nm	9800000
7ab	510 nm	10200000

Table 1. Absorbance maximums and absorptivity of **7a** and **7a'**, [M] = 50 μM, l= 1cm recorded in acetonitrile.

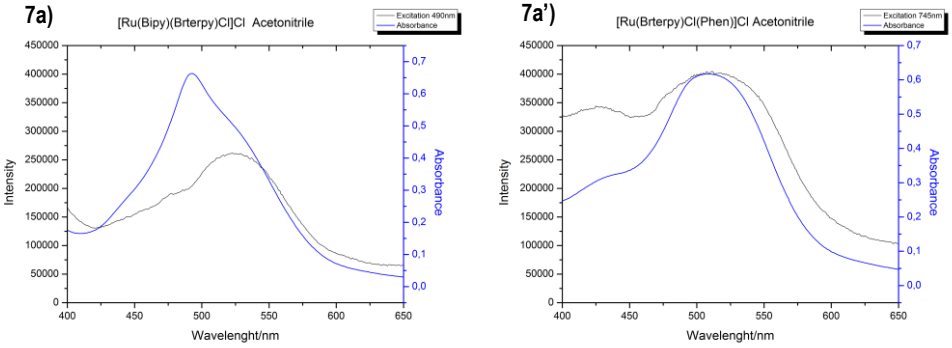

Scheme 13. Absorption and excitation spectra recorded in acetonitrile.

The absorbance and excitation spectra show similar information, and the wavelength of the maximum usually does not show significant differences (Scheme 13). It is interesting to note that [Ru(Bipy)(Brterpy)Cl]Cl (**7a**) have differences in the wavelength of the maximum can be explained by the formation of excimers [33] by studying the complex excitation spectra with different solvents (see Appendix). These peaks around 500 nm have been found to be typical of metal-to-ligand charge transfer (MLCT) in the 4'-substituted-2,2';6',2''-tpy Ru (II) complexes [34].

5.2.2. FLUORESCENCE STUDIES OF THE RUTHENIUM(II) COMPLEXES

The emission and excitation spectra of the ruthenium (II) compounds **7a** and **7a'** confirm their fluorescence features. The higher emission intensity results indicate that [Ru(Bterpy)(Cl)(Phen)]Cl has better quantum yield in contrast to [Ru(Bipy)(Bterpy)Cl]Cl.

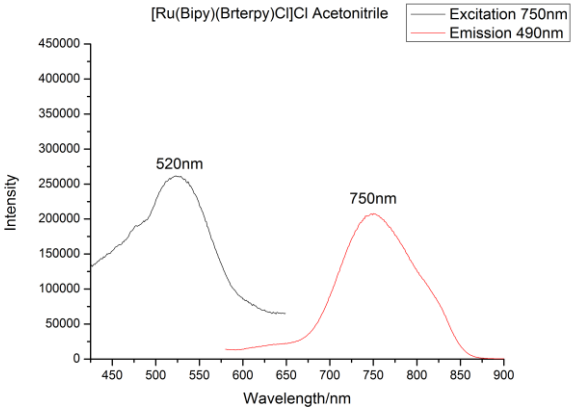

Scheme 14. Fluorescence spectra of [Ru(Bipy)(Brterpy)Cl]Cl (**7a**) C = 50 µM in acetonitrile, Stokes shift 230nm, 950 V.

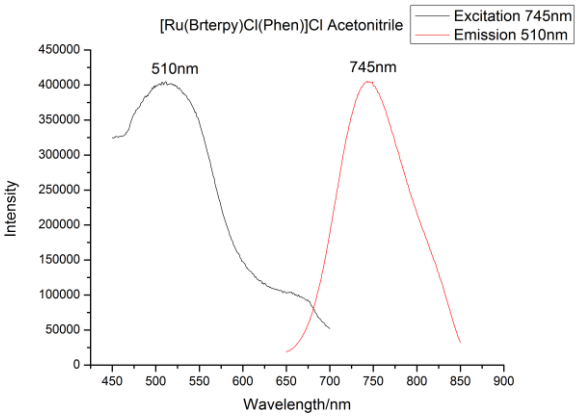

Scheme 15. Fluorescence spectra of [Ru(Brterpy)Cl(Phen)]Cl (**7a'**), [M]= 50 µM in acetonitrile, Stokes shift 235nm, 950 V.

5.2.3. DNA-BINDING STUDIES OF THE RUTHENIUM(II) COMPLEXES

DNA-cleaving properties of the complexes **7a** and **7a'** were investigated for pBR322 plasmid DNA (15 μM in base pairs) and different concentrations of the compounds (0-50 μM). All samples were incubated at 37 ºC for half an hour. Then, the even numbers were irradiated with the wavelength filter > 430 nm while the others were kept at 37 ºC. A loading buffer of 4 μl of xylene cyanol was added to the samples before injecting them to the gel of agarose in TBE buffer (Tris-borate-EDTA) at 100V for an hour and a half. The gel was then placed in a container with 150 mL of TBE and 15 μl of display buffer (SYBR Safe) and agitated overnight.

In order to investigate the interaction of ruthenium(II) complexes with DNA and its photoactivity, electrophoresis was carried out with non- irradiated and irradiated samples. Electrophoresis in agarose gel is one of the most used methods to separate and identify DNA fragments. Pure plasmid DNA gives two bands, the intense one corresponding to supercoiled DNA (Form I), while the second one is ascribed to circular nicked form (Form II). There is another form which is linear (Form III) and migrates between Form II and Form I.

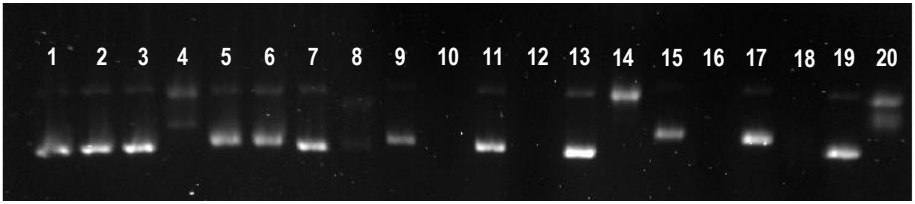

Scheme 16. Agarose gel electrophoresis images of pBR322 plasmid DNA (15 μM b.p.).Lanes 1,2: pure plasmid DNA; lanes 3,4: $[[Ru(Phen)_3]Cl_2]$ = 10 μM, lanes 5,6 [cisplatin] = 10 μM, lanes 7,8 [**5a**] 10 μM, lanes 9,10 [**7a**] 50 μM, lanes 11,12 [**7a**] 25 μM, lanes 13,14 [**7a**] 10 μM, lanes 15,16 [**7a'**] 50 μM, lanes 17,18 [**7a'**] 25 μM, lanes 19,20 [**7a'**] 10 μM.

This test revealed that the synthesised Ruthenium (II) complexes have two different effects on DNA.

It is well known that the cisplatin mechanism consists of the interaction with DNA, changing its form. However, it does not cleave the DNA. The ruthenium (II) compounds have a labile position that can interact with the DNA. This effect is observed in the electrophoresis where the complexes **7a** and **7a'** have a modified migration as cisplatin (Scheme 16, lanes 5 and 6) as seen in the non-irradiated samples (Scheme 16, lanes 9,11,13,15,17,19).

The second mechanism consists of the photosynthesized features revealed in the fluorescence studies. The irradiation of the compounds can create ROS that cleaves the Form I of the DNA into complete fragmentation (Scheme 16, lanes 10,12,16,18). In the sample with lower concentration of **7a** all the DNA is found in its circular forms, Form II (Scheme 16, lane 14). In the case of the **7a'** with lower concentration the DNA has two forms: the circular (Form II) and the linear (Form III) (Scheme 16, lane 20).

The comparison between [Ru(Brterpy)Cl(Phen)]Cl and [Ru(Bipy)(Brterpy)Cl]Cl is interesting because **7a'** (Scheme 16, lane 15) shows more cisplatin effect than **7a** (Scheme 16, lane 9), but in the irradiated samples **7a** (Scheme 16, lane 14) the DNA cleavage effect is higher than **7a'** (Scheme 16, lane 20). Also, the Brterpy (**4a**) interaction with the DNA was studied and showed non-effect (see Appendix).

The electrophoresis intensity data is proportional to the concentration of the DNA, represented in Graphic 1. A complete cleavage leads to many different fragment sizes, and there are therefore no observed bands.

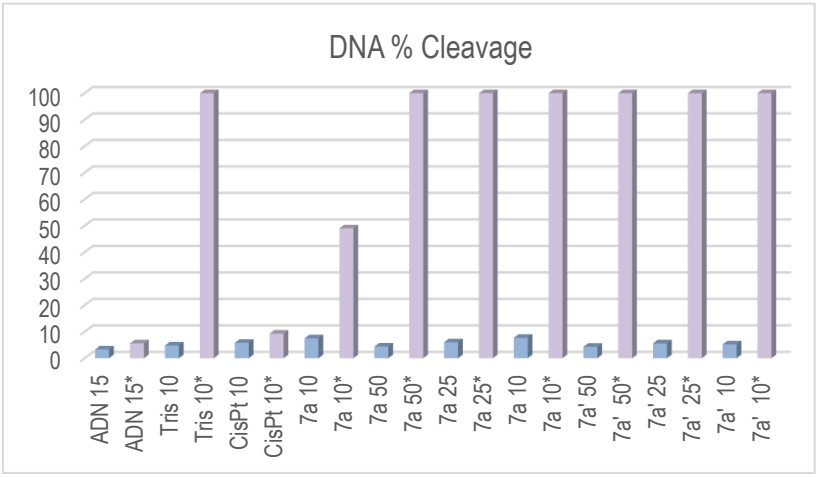

Graphic 1. Representation of the DNA % Cleavage.

There is a significant positive correlation between the photosynthesizing effect and the DNA cleavage. It is noticed that the irradiated samples are cleaved at 100% while the non-irradiated results do not have a higher percentage of cleavage. In the case of [Ru(Brterpy)Cl_3] which is also activated with the light, 49 % of DNA cleavage is observed. Furthermore, the Form II migration is modified showing a similar cisplatin interaction with the DNA (Scheme 16, lane 8).

6. EXPERIMENTAL SECTION

6.1. MATERIALS AND METHODS

The reagent and solvents used in this work were obtained from commercial sources and used as received without further purification.

Routine NMR spectra were obtained with a Mercury 400 MHz instrument. High resolution mono-^{1}H, ^{13}C{^{1}H} and bidimensional ({^{1}H-^{1}H}-COSY and {^{1}H-^{13}C}-HSCQ) NMR experiments were recorded with a Bruker Avance DMX 500 MHz instrument at 298 K. FT-IR Thermo Nicolet 330, in a 4000-400 cm^{-1} range. UV-Vis were determined on the Varian Cary-100 spectrophotometer. The Fluorescence spectra were made with Nanolog-Horiba Jobin Yvon. The instrument used for the agarose electrophoresis images was the Gel Doc EZ Imager. The elemental analyses (C,H and N) were performed at the Serveis Cientifico-Tècnics de la Universitat de Barcelona.

6.2. SYNTHESIS OF LIGANDS

6.2.1. General procedure for the synthesis of ligands

2-Acetylpyridine, an aqueous solution of KOH and NH_3 (25%) were added to a solution of 2-aminopyridine-2-carboxyaldehyde in EtOH. The resulting mixture was heated a reflux for 7h and cooled to room temperature. The solid precipitate was filtrated and dried under vacuum.

6.2.2 Synthesis of 4'-(4-bromophenyl)-2,2':6',2''-terpyridine (4a)

2-Acetylpyridine (0.391 mL ,3 mmol), KOH (0.187 g, 3 mmol) and NH_3 (0.3 mL, 25%) 4-aminobenzaldeyhde (0.278 g, 1.5 mmol) in EtOH (10 mL). Then the off-white precipitate was filtrated and washed with ethanol.

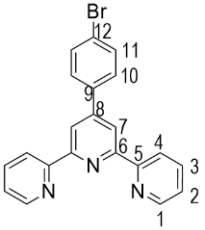

Off-white solid. Yield: 0.319 g (55%). IR (KBr, cm^{-1}): 3453, 3303, 3071, 2956, 2930, 2891, 2858, 1581, 1470. ^{1}H NMR ($CDCl_3$, 500 MHz, ppm): δ 8.73 (dd, *J* = 4.7, 1.8 Hz ,2H, H^4), 8.70 (s, 2H, H^7), 8.67 (d, *J* = 7.9 Hz, 2H, H^1), 7.88 (t, *J* = 7.7 Hz, 2H, H^2), 7.78 (d, *J* = 8.6 Hz, 2H, H^{10}), 7.64 (d, *J* = 8.7 Hz, 2H, H^{11}), 7.36 (dd, *J* = 7.5, 4.8 Hz, 2H, H^3). ^{1}H NMR (CD_3CN, 400 MHz, ppm): δ 8.72 (d, *J* = 3.9 Hz ,2H, H^4), 8.71 (s, 2H, H^7), 8.68 (d, *J* = 7.9 Hz, 2H, H^1), 7.96 (t, *J* = 7.7 Hz, 2H, H^2), 7.81 (d, *J* = 8.9 Hz, 2H, H^{10}), 7.73 (d, *J* = 8.6 Hz, 2H, H^{11}), 7.45 (dd, *J* = 7.5, 4.7 Hz, 2H, H^3). ^{13}C NMR ($CDCl_3$, 101 MHz, ppm): δ 156.3 (C^6), 156.2 (C^5), 149.3 (C^4),149.2 (C^8), 137.6 (C^9), 137.1 (C^3), 132.3 (C^{10}), 129.1 (C^{11}), 124.10 (C^2), 123,6 (C^{12}), 121.5 (C^1), 118.7 (C^7).

6.2.3 Synthesis of 4'-(4-aniline)-2,2':6',2''-terpyridine (4b)

2-Acetylpyridine (0.256 mL ,1.14 mmol), KOH (0.164 g, 1.14 mmol) and NH_3 (0.230 mL, 25%), 4-aminobenzaldeyhde (0.138 g, 1.14 mmol) in EtOH (6 mL). Then the yellow precipitate was filtrated and washed with ethanol, water and diethyl ether.

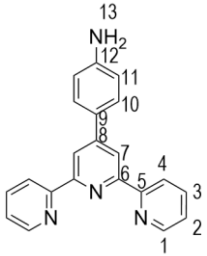

Yellow solid. Yield: 0.149 (40%). IR (KBr, cm^{-1}): 3481, 3386, 3050, 1616, 1581, 1556, 1397, 1154, 789, 568. ^{1}H NMR (DMSO-d_6, 400 MHz, ppm): δ 8.74 (d, *J* = 3.9 Hz, 2H, H^4), 8.64 (d, *J* = 7.8 Hz, 2H, H^1), 8.62 (s, 2H, H^7), 8.02 (td, *J* = 7.7, 1.9 Hz, 2H, H^3), 7.67 (d, *J* = 8.6 Hz, 2H, H^{10}), 7.50 (dd, *J* = 7.5, 4.8 Hz, 2H, H^2), 6.74 (d, *J* = 8.7 Hz, 2H, H^{11}), 5.60 (s, 2H, H^{13}). ^{13}C NMR ($CDCl_3$, 101 MHz, ppm): δ 155.4 (C^6), 155.0(C^5), 150.6 (C^8), 149.6 (C^{12}), 149.3 (C^4), 137.4 (C^3), 127.6 (C^{10}), 124.4 (C^2), 123.8 (C^9), 120.9 (C^1), 116.2 (C^7), 114.3 (C^{11})

6.2.4. Synthesis of 4'-(2-aminopyridine-3-yl)-2,2':6',2''-terpyridine (4c)

2-Acetylpyridine (1 mL ,1.14 mmol), KOH (0.467 g, 8.25 mmol), NH_3 (10 mL, 25%), 2-aminopyridine-2-carboxyaldehyde (0.070 g, 0.57 mmol), EtOH (25 mL). The resulting solution was concentrated under vacuum and the residue was passed through a silica gel column. Elution with dichloromethane/methanol (1%) produced the release of a yellow band which was collected and concentrated on a rotary evaporator.

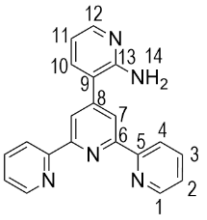

Orange oil. Yield: 0.009 g (5%). ^{1}H NMR ($CDCl_3$, 400 MHz, ppm): δ 9.15 (dd, *J* = 4.3, 2.1 Hz, 2H, H^4), 8.88 (d, *J* = 7.9 Hz, 2H, H^{14}), 8.75 (m, 2H, H^1), 8.74 (s, 2H, H^7), 8.32 (d, *J* = 8.5 Hz, 2H, H^2), 8.23 (dd, *J* = 8.1, 2.1 Hz, 2H, H^3), 7.89 (td, *J* = 7.8, 1.9 Hz, 1H, H^{12}), 7.50 (dd, *J* = 8.1, 4.2 Hz, 1H, H^{11}), 7.39 (dd, *J* = 6.3, 7.7 Hz, 1H, H^{10}). ^{13}C NMR ($CDCl_3$, 101 MHz, ppm): δ 159.7 (C^{13}), 156.2 (C^6), 155.8 (C^5), 154.2 (C^8), 149.5 (C^1), 138.2 (C^2), 137.4 (C^3), 137.3 (C^{12}), 125.1 (C^{10}), 123.3 (C^9), 123.0 (C^4), 122.6 (C^{11}), 120.6 (C^7).

6.2.5 Synthesis of 4'-(*N*-(2-hydroxyethyl)-*N*-methyl)-2,2':6',2''-terpyridine (4d)

2-Acetylpyridine (0.137 mL ,1.22 mmol), KOH (0.068 g, 1.22 mmol) and NH_3 (1.37 mL, 25%), N-(2-hydroxyethyl)-N-methyl-4-benzaldehyde (0.102 g, 0.57 mmol) in EtOH (5 mL). The resulting oil was purified by SiO_2 column using ethyl acetate:hexane (1:4) as eluent and resulted in the starting aldehyde and its reduced form.

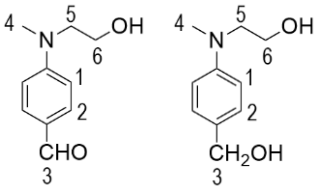

Oil. ^{1}H NMR aldehyde ($CDCl_3$, 400 MHz, ppm): δ 9.75 (s, 2H, H^3), 7.74 (d, *J* = 9.1 Hz, 2H, H^1), 6.76 (d, *J* = 9.1 Hz, 1H, H^2) 4.28 (t, *J* = 6.0 Hz, 2H, H^5), 3.70 (t, *J* = 6.0 Hz, 2H, H^5), 3.09 (s, 3H, H^4). ^{1}H NMR alcohol ($CDCl_3$, 400 MHz, ppm): δ 7.22 (d, *J* = 8.8Hz, 2H, H^1), 6.78 (d, *J* = 8.8 Hz, 2H, H^2), 4.40 (s, 2H, H^3), 3.81 (t, *J* = 5.8 Hz, 2H, H^5), 3.50 (q, *J* = 7.0 Hz, 2H, H^6), 3.47 (t, *J* = 5.7 Hz, 2H, H^2), 2.96 (s, 3H, H^4).

6.2.6 Synthesis of 4'-(naphthalen-2-ylmethoxy)-2,2':6',2''-terpyridine (4e)

2-naphthalnemethanol (0.100 g, 0.632 mmol) was added to a suspension of KOH (0,039 g, 3.160 mmol) in DMSO (5 mL). The 4'-chloro-2,2':6',2''-terpyridine (0.165 g, 0.620 mmol) was added to the mixture after 30 minutes of stirring at 70 ºC. It was then further stirred for 4 hours at 70 ºC. The resulting mixture was poured into 100 mL of cold water with ice. The white precipitate was filtrated and washed with cold water and chloroform (3 x 5 mL) then dried under reduced pressure.

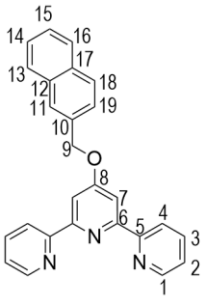

Off-white solid. Yield: 0.153 g (63%). IR (KBr, cm^{-1}): 3421, 3053, 3012, 1582, 1556, 1350, 1005. ^{1}H NMR ($CDCl_3$, 400 MHz, ppm): δ 8.72 (d, *J* = 5.2 Hz, 2H, H^4), 8.63(d, *J* = 7.7 Hz, 2H, H^1), 8.17 (s, 2H, H^7), 7.97 (s, 1H, H^{11}), 7.88 (m, 5H, H^3, H^{18}, H^{19}), 7.59 (d, *J* = 8.3 Hz, 1H, H^{16}), 7.50 (m, 2H, H^2), 7.33 (dd, *J* = 7.7, 4.7 Hz, 2H, H^{14}), 5.50 (s, 2H,H^9). ^{13}C NMR ($CDCl_3$, 101 MHz, ppm): δ 166.2 (C^8), 156.8 (C^6), 154.8 (C^5), 149.3 (C^4), 137.4 (C^3), 133.9 (C^{10}), 132.8 (C^{12}), 126.4 (C^{11}), 126.2 (C^2), 120.9 (C^1), 107.2 (C^7), 69.6 (C^9).

6.3. SYNTHESIS OF RUTHENIUM COMPLEXES

6.3.1. Synthesis of $RuCl_2(dmso)_4$

An amount of $RuCl_3 \cdot 3H_2O$ (1 g, mmol) was refluxed in DMSO (6 mL) with intense heating for 15 minutes. The mixture was cooled to room temperature and two drops of H_2O and acetone (10 mL) were added. The yellow precipitate was filtrated, the red-brown mother liquor was left standing for 3 days and yellow crystals deposited.

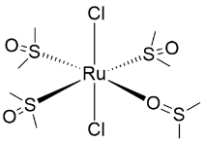

Yellow solid. Yield: 1.035 g (57%) IR (KBr, cm^{-1}): 2997, 1306, 1127, 1096, 1023, 984, 975, 923, 678. ^1H NMR ($CDCl_3$, 400 MHz, ppm): δ 3.53, 3.50, 3.47, 3.44, 3.41,3.33 (Me of DMSO, S-Ru linked), 2.73 (Me of DMSO, O-Ru linked), 2.62 (Me of free DMSO), ratio S-Ru:O-Ru 4:1

6.3.2. General procedure for the synthesis of $[Ru(Rterpy)Cl_3]$ complexes

The $RuCl_3 \cdot 3H_2O$ was dissolved in ethanol (30 mL) and the solution was refluxed for 2 h under nitrogen atmosphere. The solution color changed from brown to dark green. Then the stoichiometric amount of ligand was added and refluxed for 5 more hours. The mixture was cooled at room temperature and a dark brown solid precipitated. This was filtrated and washed with ethanol, diethyl ether and dried under vacuum.

6.3.2.1. Synthesis of $[Ru(Brterpy)Cl_3]$ (5a)

The reagent amounts used in the synthesis were 0.131 g (0.5 mmol) $RuCl_3 \cdot 3H_2O$ and 0.194 g (0.5 mmol) of 4'-(4-bromophenyl)-2,2':6',2''-terpyridine.

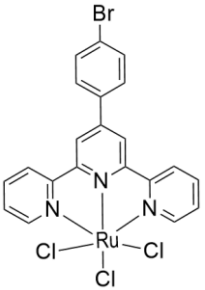

Dark brown solid. Yield: 0.198 g (66%). Elemental analysis calculated for $C_{21}H_{14}N_3BrCl_3Ru \cdot H_2O$ (%): C (41.10), H (2.62), N (6.85); found: C (41.2), H (2.4), N (6.8). IR (KBr, cm^{-1}): 3452, 3066, 1606, 1464, 1002, 789.

6.3.2.2. Synthesis of [Ru(Anilineterpy)Cl_3] (5b)

In this synthesis 0.131 g (0.5 mmol) of $RuCl_3 \cdot 3H_2O$ and the stoichiometric amount of 4'-(4-aniline)-2,2':6',2''-terpyridine 0.162 g (0.5 mmol) were used.

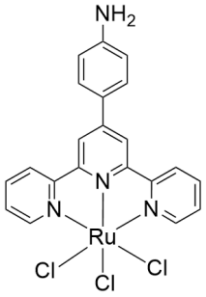

Dark brown solid. Yield: 0.180 (68%). Elemental analysis calculated for $C_{21}H_{16}N_4Cl_3Ru$ (%): C (47.43), H (3.03), N (10.54); found: C (33.3), H (3.1), N (6.8). IR (KBr, cm^{-1}): 3424, 3215, 3068, 2917, 1600, 1556.

6.3.2.3. Synthesis of [Ru(Nterpy)Cl_3] (5e)

The amounts used in the synthesis were 0.096 g (0.366 mmol) of $RuCl_3 \cdot 3H_2O$ and 0.143 g (0.366 mmol) of 4'-(4-aniline)-2,2':6',2''-terpyridine.

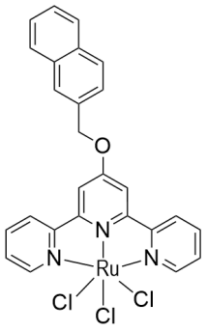

Dark brown solid. Yield: 0.201 g (92 %). Elemental analysis calculated for $C_{26}H_{19}N_3OCl_3Ru$ (%): C (52.32), H (3.19), N (7.04); found: C (37.5), H (3.0), N (5.5).

6.4.1. General procedure for the synthesis of [Ru(Nterpy)(Rterpy)]$(PF_6)_2$ complexes

A stoichiometric amount Rterpy (**4a**,**4b**) was added in a methanolic solution of [Ru(Nterpy)Cl_3] (**5e**) with 5 drops of N-methylmorpholine and refluxed under nitrogen atmosphere for 8 hours. After this, the hexafluorophosphate was added and the solid precipitate was filtrated. The products of this synthesis resulted in a mixture that was difficult to purify.

6.5. General procedure for the synthesis of [RuCl(N,N')(Rterpy)]Cl complexes, Rterpy = 4a, 4b; N,N' = Bipy, Phen

A weighed amount of [Ru(Rterpy)Cl_3], where Rterpy = **4a** or **4b** was suspended in an ethanol:water (3:1, 20 mL) mixture with LiCl (10 eq.) and triethylamine (3 eq.) under nitrogen atmosphere. The bidentate ligand was then added and refluxed for 7 h. The dark precipitate was washed with acetone.

6.5.1. Synthesis of [Ru(Bipy)(Brterpy)Cl]Cl (7a)

For the obtention of **7a** were used the following reagent amounts: [Ru(Brterpy)Cl_3] (0.149 g, 0.25 mmol), LiCl (0.106 g, 2.5mmol), triethylamine (105 µL, 0.75 mmol) and 2,2'-bipyridine (0.047 g, 0.25 mmol).

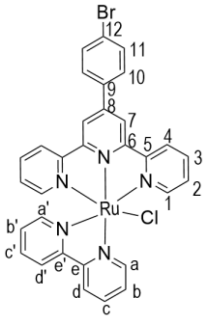

Brown solid. Yield: 0.059 g (35%). IR (KBr, cm^{-1}): 3379, 3053, 1600, 1464, 1426, 786. ^{1}H NMR (CD_3CN, 400 MHz, ppm): δ 10.24 (d, *J* = 5.1 Hz, 1H, H^a), 8.74 (s, 2H, H^7), 8.61 (d, *J* = 8.2 Hz, 1H, H^d), 8.52 (d, *J* = 8.1 Hz, 2H, H^4), 8.31 (d, *J* = 8.2, 1H, $H^{d'}$), 8.27 (t, *J* = Hz, 1H, H^c), 8.04 (d, *J* = 8.7 Hz, 2H, H^{10}), 7.87 (m, 5H, H^{11}, H^3, H^b), 7.69 (d, *J* = 6.3 Hz, 3H, H^1, $H^{c'}$), 7.36 (d, *J* = 5.4 Hz, 1H, $H^{a'}$), 7.29 (t, *J* = 5.9 Hz, 2H, H^2). ^{13}C NMR (CD_3CN, 101 MHz, ppm): δ 159.7 (C^6), 159.2 (C^5), 153.4 (C^e), 153.3 ($C^{e'}$), 145.7 (C^8), 139.1 (C^9), 138.0 (C^{11}), 137.5 (C^c), 137.4 ($C^{c'}$), 136.5 (C^1), 133.5 (C^3), 130.7(C^a), 130.5 (C^{10}), 128.5 ($C^{a'}$), 128.3 (C^2), 127.9 (C^b), 127.0 ($C^{b'}$), 124.7 (C^4), 124.4 (C^d),124.2 ($C^{d'}$), 122.6 (C^{12}), 121.4 (C^7). HRMS (ESI) calculated: 680.93 *m/z*; found 682.09 *m/z*.

6.5.2. Synthesis of [Ru(Brterpy)Cl(Phen)]Cl (7a')

In the synthesis 0.100 g (0.168 mmol) of [Ru(Brterpy)Cl_3], 0.071 g (1.68 mmol) of LiCl, 70 µL (0.504 mmol) of triethylamine and 0.036 g (0.168 mmol) of 1,10-phenantroline were used.

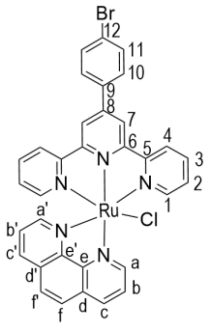

Brown solid. Yield: 0.080 g (68%). IR (KBr, cm^{-1}): 3408, 3348, 2917, 1416, 1081, 837. ^{1}H NMR (CD_3CN, 400 MHz, ppm): δ 10.45 (d, *J* = 6.6 Hz, 1H, H^a), 8.82 (d, *J* = 8.2 Hz, 1H, H^d), 8.78 (s, 2H, H^7), 8.53 (d, *J* = 8.1 Hz, 2H, H^4), 8.33 (m, 2H, H^b, $H^{d'}$), 8.23 (d, *J* = 9.4 Hz, 1H, $H^{c'}$), 8.08 (t, *J* = 8.9 Hz, 3H, H^{10}, H^c), 7.87 (m, 4H, H^{11}, H^3), 7.71 (d, *J* = 6.7 Hz, 1H, $H^{a'}$), 7.54 (d, *J* = 5.6 Hz, 2H, H^1), 7.29 (dd, *J* = 8.2, 5.4 Hz, 1H, $H^{b'}$), 7.15 (t, *J* = 7.2 Hz, 2H, H^2). ^{13}C NMR (CD_3CN, 101 MHz, ppm): δ 159.6 (C^5), 159.3 (C^6), 153.5 ($C^{a'}$), 153.4 (C^a), 137.9 (C^{11}), 136.4 (C^c), 135.4 ($C^{c'}$), 133.5 (C^3),131.8 (C^{12}), 130.5 (C^{10}), 128.9 (C^f), 128.5 ($C^{f'}$), 128.1 (C^2), 126.8 (C^b), 125.7 ($C^{b'}$), 124.6 (C^4), 121.0 (C^7). HRMS (ESI) calculated: 704.99 *m/z*; found 706.06 *m/z*.

6.5.3. Synthesis of [Ru(Anilineterpy)(Bipy)Cl]Cl (7b)

The amounts used in the synthesis were 0.096 g (0.181 mmol) of [Ru(Anilineterpy)Cl_3], 0.077 g (1.81 mmol) of LiCl, 76 µL (0.543 mmol) of triethylamine and 0.034 g (0.181 mmol) of 2,2'-bipyridine. The product of this synthesis resulted in a mixture of [Ru(Anilineterpy)(Bipy)Cl]Cl impurified with [Ru(Bipy)$_3$]Cl_2, difficult to purify.

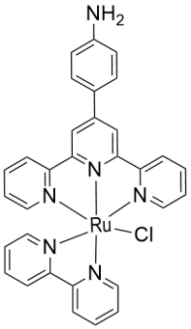

Brown solid. Yield: 0.031 g (28%). HRMS (ESI) calculated: 617.06 *m/z*; found 617.20 *m/z* and 279.05 *m/z*.

6.5.4. Synthesis of [Ru(Anilineterpy)Cl(Phen)]Cl (7b')

The reagent amounts used in the synthesis were 0.096 g (0.181 mmol) of [Ru(Anilineterpy)Cl_3], 0.077 g (1.81 mmol) of LiCl, 77 µL (0.543 mmol) of triethylamine and 0.033 g (0.181 mmol) of 1,10-phenantroline. The product of this synthesis resulted in a mixture of [Ru(Anilineterpy)Cl(Phen)]Cl impurified with [Ru(Phen)$_3$]Cl_2.

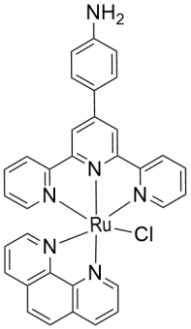

Brown solid. Yield: 0.061 g (53%). HRMS (ESI) calculated: 641.91 *m/z*; found 641.16 *m/z* and 320.95 *m/z*.

7. CONCLUSIONS

In this project, the synthesis of the ligands 4'-(4-bromophenyl)-2,2':6',2''-terpyridine (**4a**), 4'-(4-aniline)-2,2':6',2''-terpyridine (**4b**), 4'-(2-aminopyridine-3-yl)-2,2':6',2''-terpyridine (**4c**) and the ruthenium (II) complexes [Ru(Bipy)(Brterpy)Cl]Cl (**7a**), [Ru(Brterpy)Cl(Phen)]Cl (**7a'**) were achieved and characterized. After washing the brown precipitate from these reactions with acetone, the pure complexes **7a** and **7a'** were obtained. The characterization data (^{1}H NMR, ^{13}C{^{1}H} NMR, COSY, HSQC, MS) agree with the proposed structures.

UV-Vis showed that the maximum absorbance wavelength of the complexes (**7a**,**7a'**) is around 500 nm. This value is in line with the typical tpy absorbance. This result was used in the further fluorescence studies, on emission spectra which confirmed the fluorescence activity of these ruthenium (II) complexes.

The evidence from the electrophoresis study suggests that both ruthenium (II) complexes (**7a**,**7a'**) have two different mechanisms to interact with DNA. The first is by acting like cisplatin and modifying the DNA structure. The second consists of activation of the complex with light, which results in high values of DNA cleavage.

Our work has led us to conclude that the two compounds synthesized have interesting fluorescence properties that activate the DNA cleavage therefore they can act as photosensitizers. Further experimental investigations are needed to estimate their pharmacological activity by using the interesting photosensitizer features and applying the phototherapy methodology.

8. REFERENCES AND NOTES

1. G. B. Kauffman, R. Pentimalli, S. Doldi, M. D. Hall, *Platinum metals review*, **2010**, Vol. 54, 250-256.
2. B. Rosenberg, L. Van Camp, E. B. Grimely, A. J. Thomson, The Journal of Biological Chemistry, **1967**, Vol. 242, 1347-1352.
3. B. Rosenberg, L. Van Camp, *Cancer Research*, **1970**, Vol. 30, 1799-1802.
4. M. A Skowron, M. Melnikoya, J.G. H van Roermund, A. Romano, P. Albers, J. Thomale, W. A. Schulz, G. Niegisch, M. J. Hoffmann, *International Journal Molecular Science*, **2018**, Vol. 19, 590-507.
5. R. Oun, Y.E. Moussa, *Dalton Trans*, **2018**, Vol. 47, 6645-6653.
6. T. Boulikas, *Expert Opinion on Investigational*, **2009**, Vol. 18, 1197-1218.
7. H. Cui, R. Goddard, K. R. Pörschke, A. Hamacher, M.U. Kassack, *Inorganic Chemistry*, **2014**, Vol. 53, 3371-3384.
8. N. J. Wheate, S. Walker, G. E. Craig, R. Oun, *Dalton Transactions,* **2010**, Vol. 39, 8113-8127.
9. S.Ghosh, *Bioorganic Chemistry*, **2019**, Vol. 88, 102925.
10. U. Ndagi, N. Mhlongo, M. E. Soliman, *Drug Design*, *Development and Therapy*, **2017**, Vol. 11, 599-616.
11. E. J. Anthony, E. M. Bolitho, H. E. Bridgewater, O.W. L. Carter, J. M. Donnelly, C. Imberti, E. C. Lant, F. Lermyte, R. J. Needham, M. Palau, P. J. Sadler, H. Shi, F. X. Wang, W. Y. Zhang, Z. Zhang, *Chemical Science*, **2020**, Vol. 11, 12888-12917.
12. S. Page, *Education in Chemistry*, **2012**, Vol. 10, 26-29.
13. E. Alessio, Z. Guo, *European Journal of Inorganic Chemistry*, **2017**, Vol. 2017, 1549-1560.
14. C. S. Allardyce, P. J. Dyson, *Dalton Transactions*, **2016**, Vol. 45, 3201-3209.
15. S. Thota, D. A. Rodrigues, D. C. Crans, E. J. Barreiro, *Journal of Medicinal Chemistry*, **2018**, Vol. 61, 5805-5821.
16. C. Mari, V. Pierroz, S. Ferrari, G. Gasser, *Chemical Science*, **2015**, Vol. 6, 2660-2686.
17. H. Y. Ding, X. S. Wang, L. Q. Song, J. R. Chen, J. H. Yu, C. Li, B. W. Zhang, *Journal of Photochemistry and Photobiology*, **2006**, Vol. 177, 286-294.
18. H. J. Yu, S. M. Huang, L. Y. Li, H. N. Jia, H. Chao, Z. W. Mao, J. Z. Liu, L. N. Ji, *Journal Inorganic Biochemistry*, **2009**, Vol. 103, 881-890.
19. J. Karges, S. Kuang, F. Maschietto, O. Blacque, I. Ciofini, H. Chao, G. Gasser, *Nature Communications*, **2020**, Vol. 11, 1-13.
20. J. Li, T. Chen, *Coordination Chmistry Reviews*, **2020**, Vol. 418, 213355.
21. S. Monro, K. L. Colón, H. Yin, J. Roque III, P. Konda, S. Gujar, R. P. Thummel, L. Lilge, C. G. Cameron, S. A. McFarland, *Chemical Reviews*, **2019**, Vol. 119, 797-828.
22. L. A. Saghatforoush, L. Valencia, F. Chalabian, Sh. Ghammamy, *Bioinorganic Chemistry Applications*, **2011**, 1-7.
23. M. A. Martínez, M. P. Carranza, A. Massaguer, L. Santos, J. A. Organero, C. Aliende, R. de Llorens, I. Ng-Choi, L. Feliu, M. Planas, A. M. Rodríguez, B. R. Manzano, G. Espino, F. A. Jalón, *Inorganic Chemistry*, **2017**, Vol. 56, 13679-13696.
24. M. M. Elnagar, S. Samir, Y. M. Shaker, A. A. Abdel-Shafi, W. Sharmoukh, M. S. Abdel-Aziz, K. S. Abou-El-Sherbini, Applied Organometallic *Chemistry*, **2020**, Vol. 35, 1-16.

25. J. Grau, F. Brissos, J. Salinas-Uber, A. B. Caballero, A. Caubet, O. Roubeau, L. Korrodi-Gregórco, R. Pérez-Tomás, P. Gàmez, *Dalton Transactions*, **2015**, Vol. 44, 16061-16072.
26. G. W. V. Cave, C. L. Raston, *Chemical Communications*, **2000**, 2199-2200.
27. V. Mahalingam, N. Chitrapriya, F. R. Fronczek, K. Natarajan, *Polyhedron*, **2008**, Vol. 27, 1917-1924.
28. S. Evans, Wilkinson, *Dalton Trans*, **1973**, Vol.204,
29. A. Anthonysamy, S. Balasubramanian, V. Shanmugaiah, N. Mathivanan, *Dalton Trans.actions*, **2008**, 2136–2143.
30. T. Ezhilarasu, A. Sathiyaseelan, P. T. Kalaichelvan, S. Balasubramanian, *Journal of Molecular Structure*, **2017**, Vol. 1134, 265-277.
31. J. Karges, S. Kuang, F. Maschietto, O. Blacque, I. Ciofini, H. Chao, G. Gasser, *Nature Communications*, **2020**, Vol. 11, 1-13.
32. M. M. Milutinović, A. Rilak, I. Bratsos, O. Klisurić, M. Vraneš, N. Gligorijević, S. Radulović, Z. D. Bugarčić, *Jouran of Inorganic Biochemistry,* **2017**, Vol. 169, 1-12.
33. H. Zeng, C. Liu, M. Kira, Y. Segawa, *Journal of Physics B: Atomic, Molecular and Optical Physics*, **1999**, Vol. 32, L225-L230.
34. M. M. Elnagar, S. Samir, Y. M. Shaker, A. A. Abdel-Shafi, W. Sharmoukh, M. S. Abdel-Aziz, K. S. Abou-El-Sherbini, *Applied Organometallic Chemistry*, **2021**, Vol. 35, 1-16.

9. ACRONYMS

IR: Infrared

NMR: Nuclear magnetic resonance

DNA: Deoxyribonucleic acid

UV-Vis: UltraViolet-Visible

FDA: US Food and Drug Administration

d(GpG): Deoxiguanylyl(3'-5 ')-2'-deoxyguanosine

d(ApG): Deoxyadenylyl-(3'-5')-deoxyguanosine

Ru: ruthenium

Cisplatin: *cis*-diamminedichloridoplatinum(II)

ROS: Reactive oxygen species

PSs: photosensitizers

PDT: photodynamic therapy

MLCT: transference metal-to-ligand

tpy: "2,2';6',2''-terpyridine

DMSO: dimethyl sulfoxide

KOH: potassium hydroxide

N_2: molecular nitrogen

PF_6: hexafluorophosphate

Bipy: 2,2'-bipyridine

Phen: 1,10-phenantroline

NH_3: ammonia

EtOH: ethanol

APPENDIX

APPENDIX 1: NMR SPECTRA

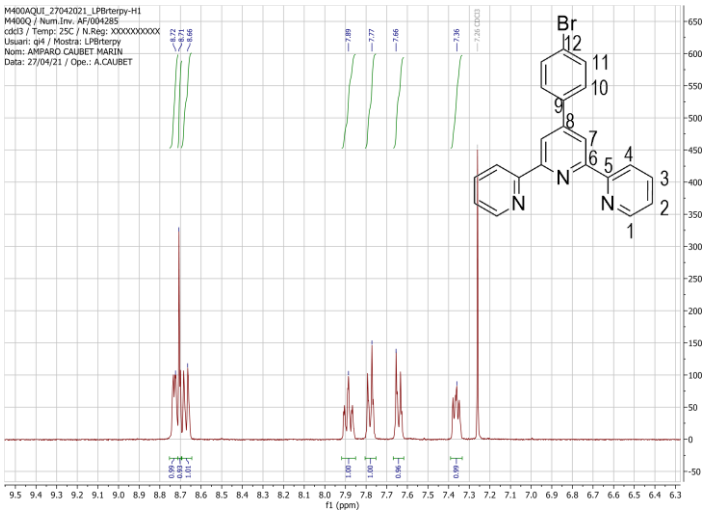

Scheme 1. ^{1}H NMR spectrum of **4a** in chloroform-d_6

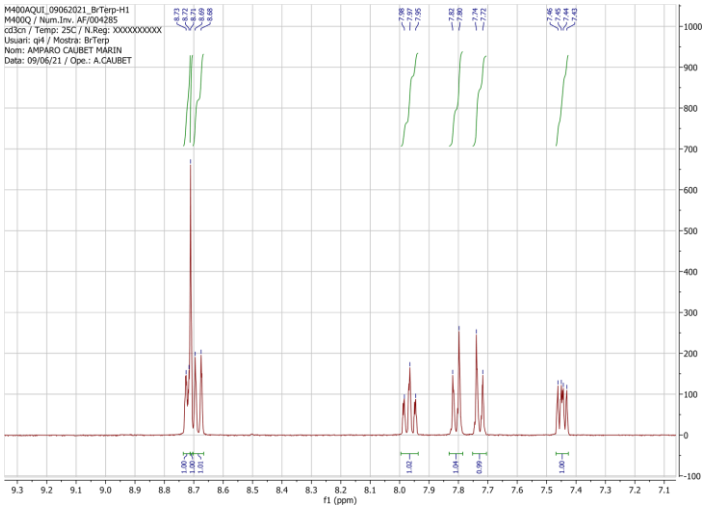

Scheme 2. ^{1}H NMR spectrum of **4a** in acetonitrile-d_3

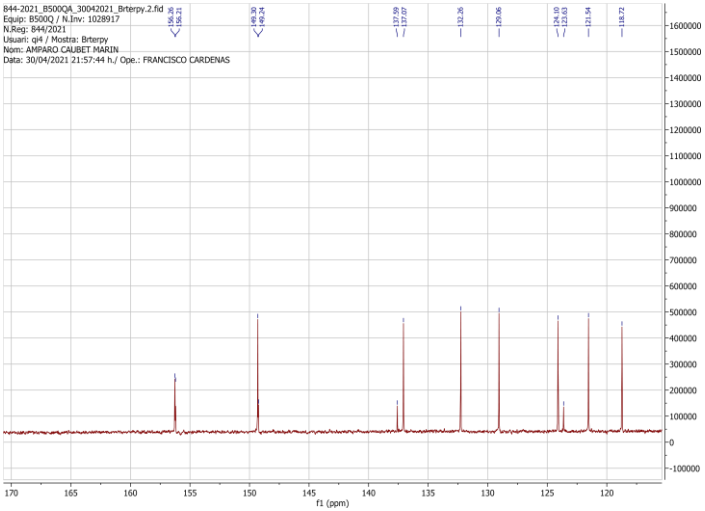

Scheme 3. $^{13}C\{^{1}H\}$ NMR spectrum of **4a** in chloroform-d_6

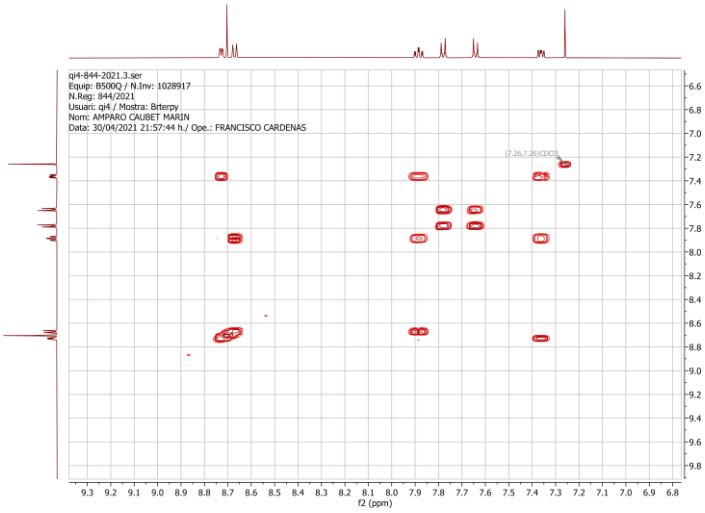

Scheme 4. $\{^{1}H,^{1}H\}$-COSY spectrum of **4a** in chloroform-d_6

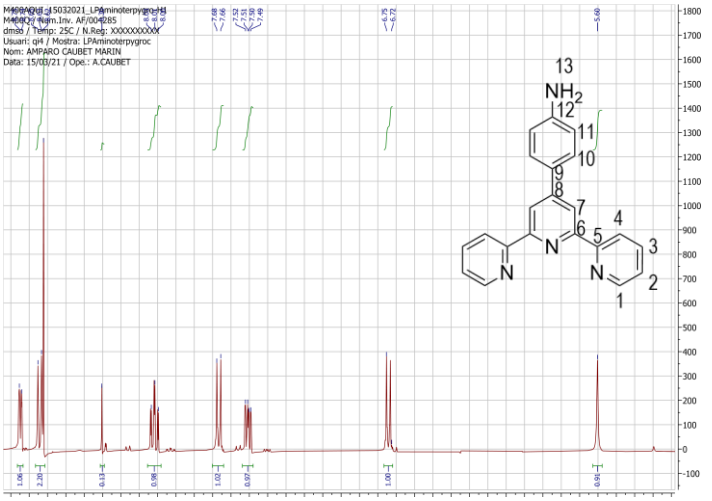

Scheme 5. ^{1}H NMR spectrum of **4b** in chloroform-d_6

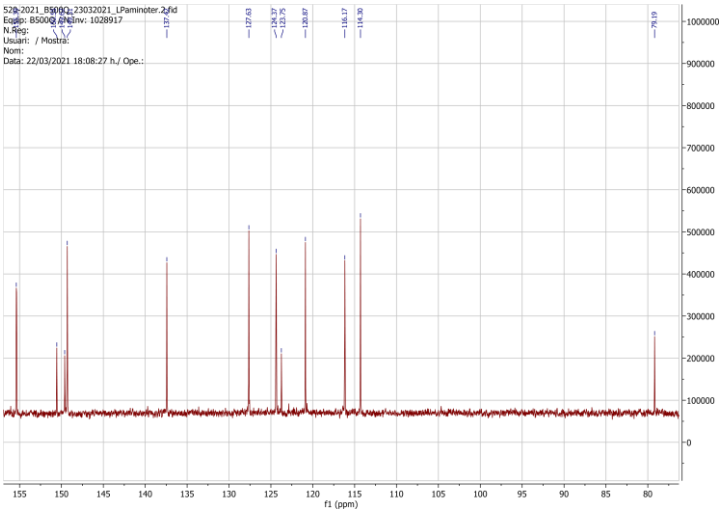

Scheme 6. ^{13}C{^{1}H} NMR spectrum of **4b** in chloroform-d_6

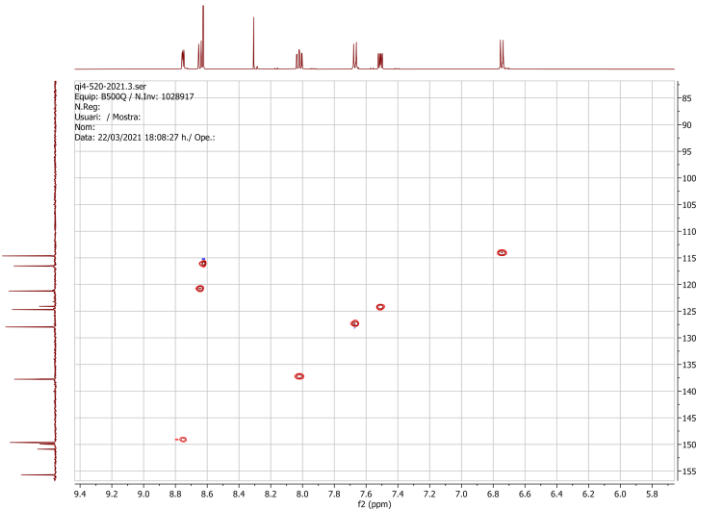

Scheme 7. {^{1}H-^{13}C{^{1}H}}-HSQC spectrum of **4b** in in chloroform-d$_6$

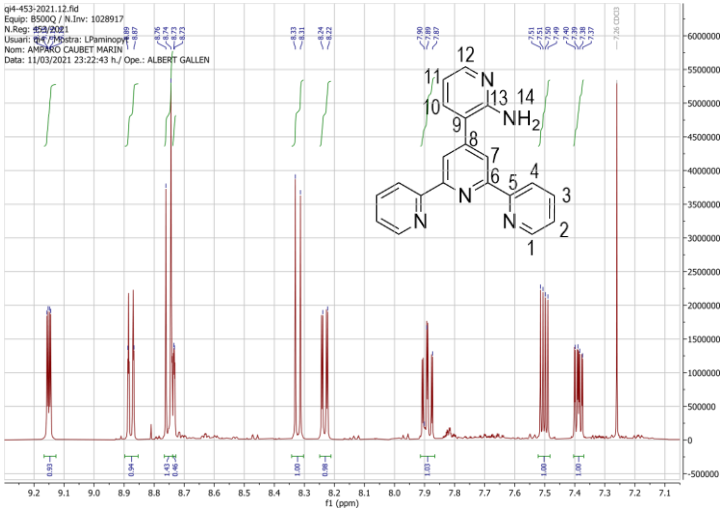

Scheme 8. ^{1}H NMR spectrum of **4c** in in chloroform-d$_6$

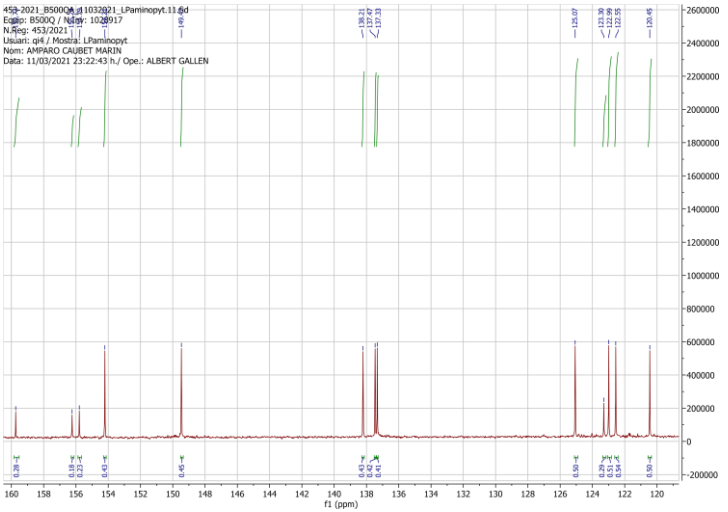

Scheme 9. $^{13}C\{^{1}H\}$ NMR spectrum of **4c** in chloroform-d_6

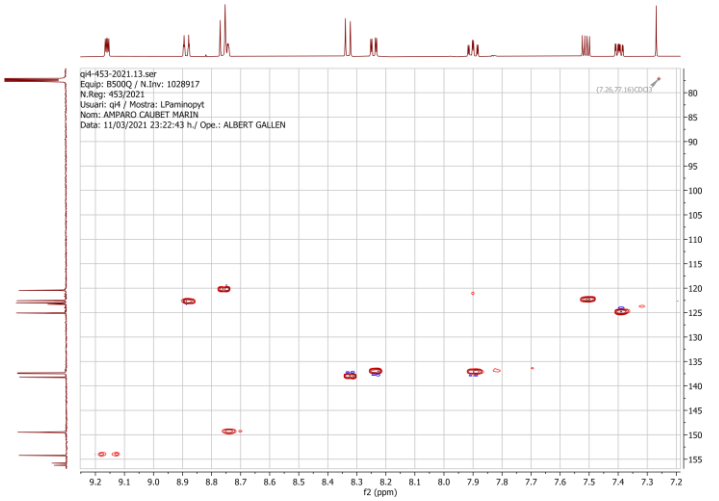

Scheme 10. $\{^{1}H\text{-}^{13}C\{^{1}H\}\}$-HSQC spectrum of **4c** in chloroform-d_6

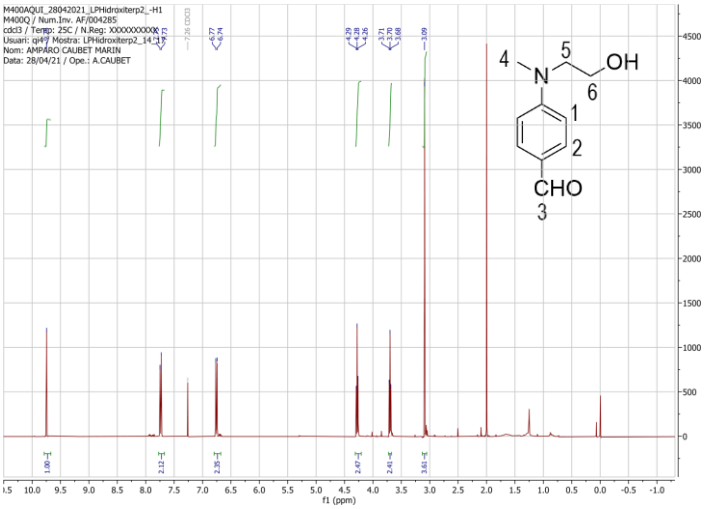

Scheme 11. ^{1}H NMR spectrum of the aldehyde **1d** in chloroform-d_6

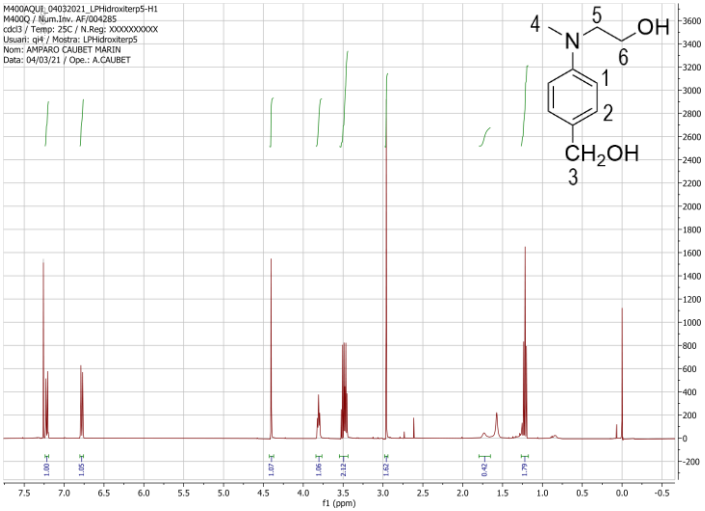

Scheme 12. ^{1}H NMR spectrum **1d** reduced to alcohol in chloroform-d_6

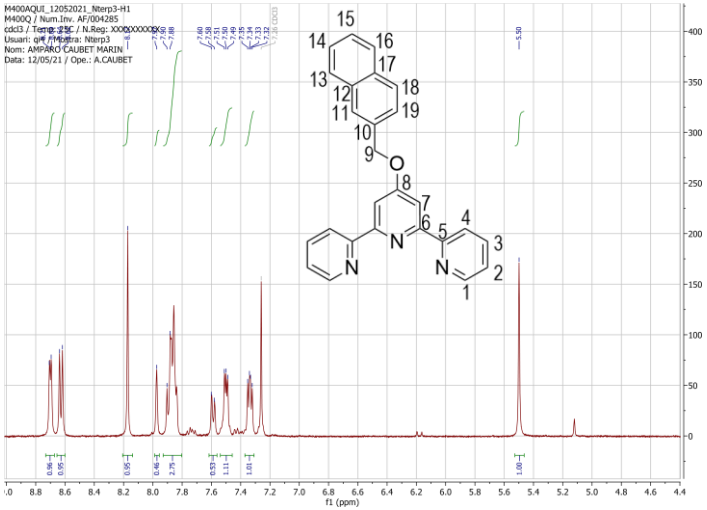

Scheme 13. ^{1}H NMR spectrum of **4e** in chloroform-d_6

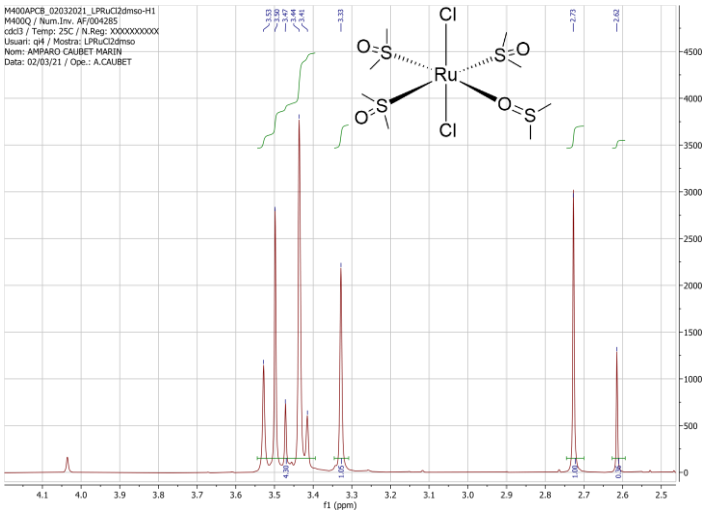

Scheme 14. ^{1}H NMR spectrum of $RuCl_2(dmso)_4$ in chloroform-d_6

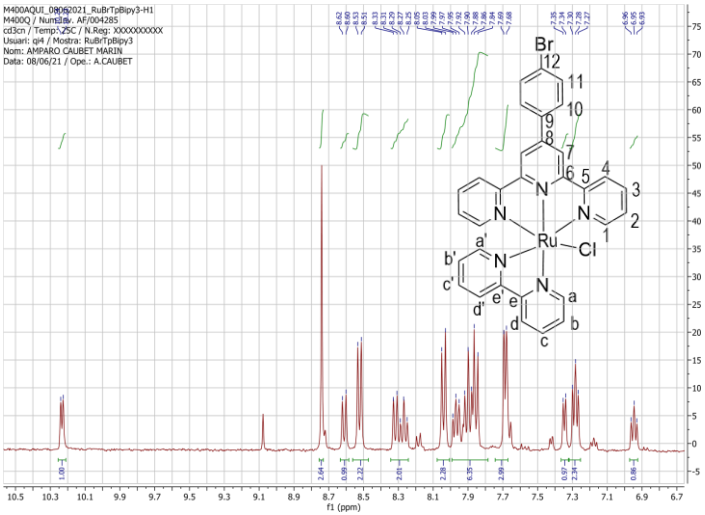

Scheme 15. ^{1}H NMR spectrum of **7a** in acetonitrile-d$_3$

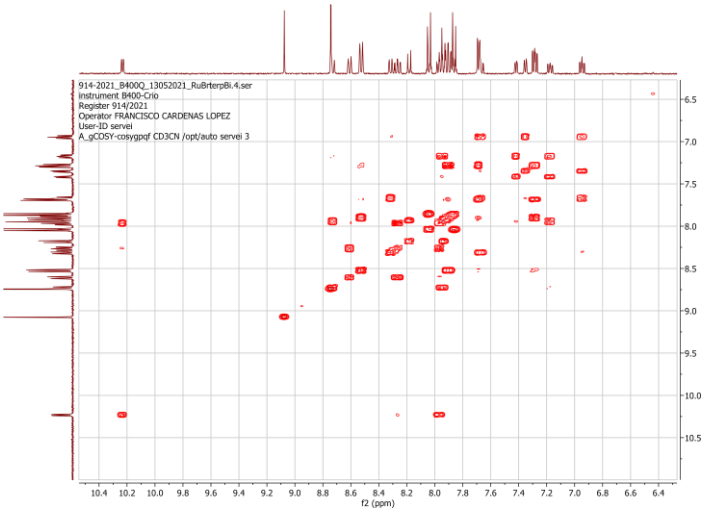

Scheme 16. {^{1}H,^{1}H}-COSY spectrum of **7a** acetonitrile-d$_3$

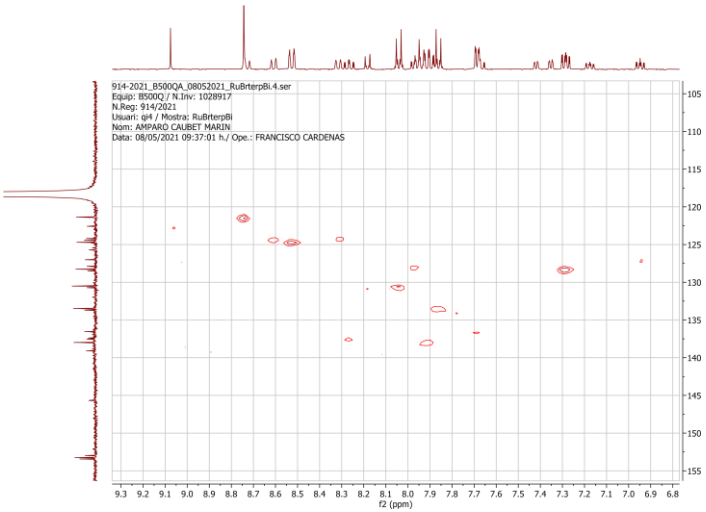

Scheme 17. {^{1}H-^{13}C{^{1}H}}-HSQC spectrum of **7a** acetonitrile-d_3

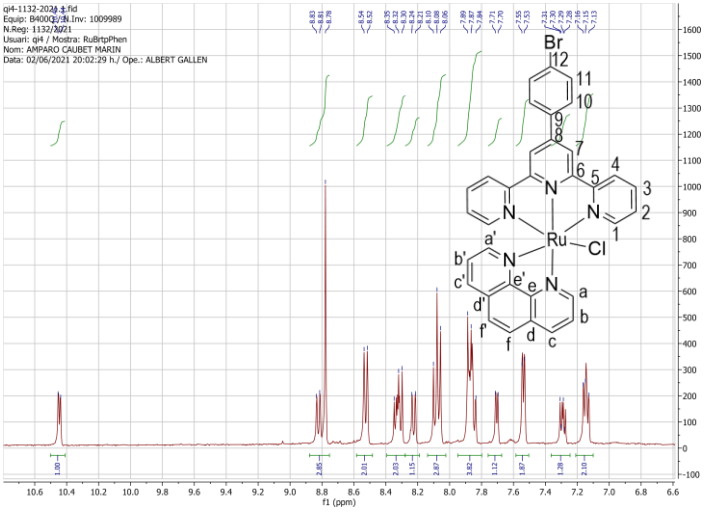

Scheme 18. ^{1}H NMR spectrum of **7a'** in acetonitrile-d_3

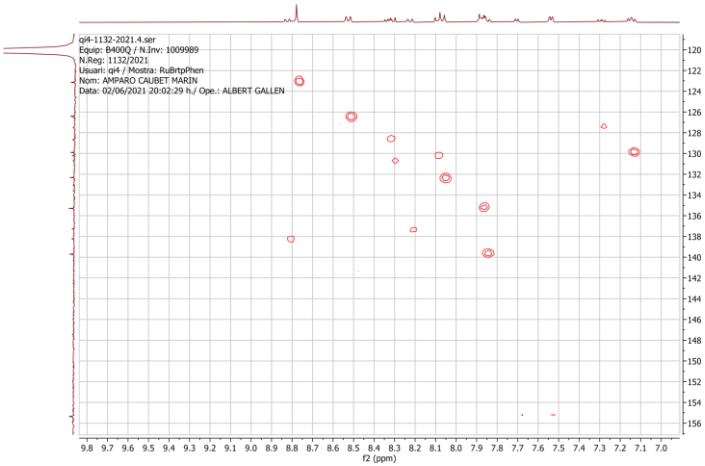

Scheme 19. {^{1}H-^{13}C{^{1}H}}-HSQC spectrum of **7a'** acetonitrile-d$_3$

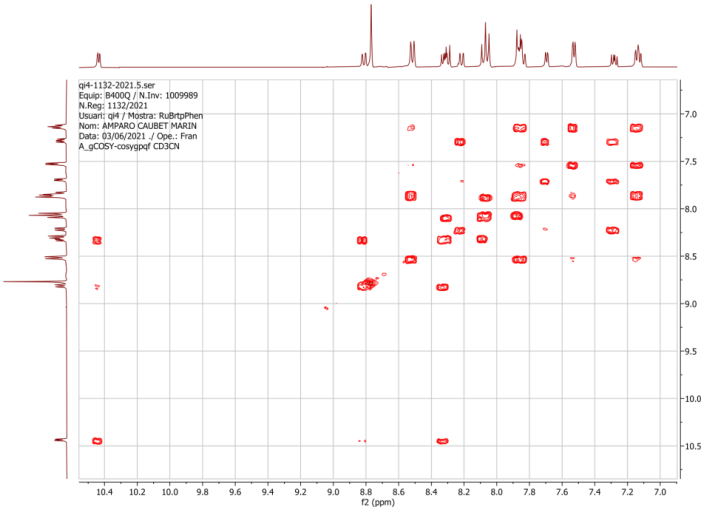

Scheme 20. {^{1}H,^{1}H}-COSY spectrum of **7a'** in acetonitrile-d$_3$

APPENDIX 2: IR SPECTRUM OF 4'-(4-BROMOPHENYL)-2,2':6',2''-TERPYRIDINE (4A)

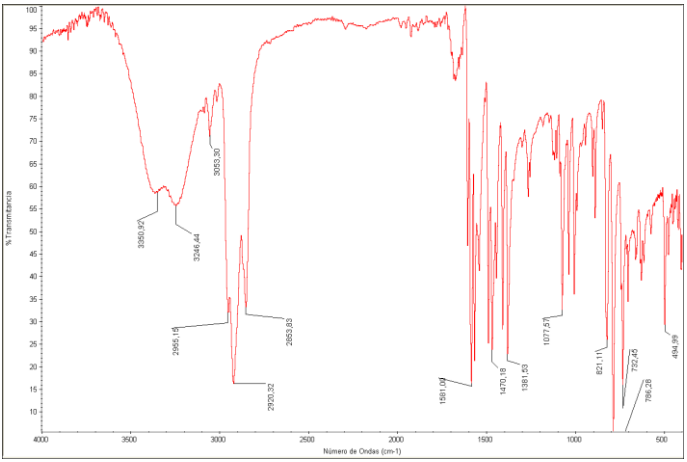

Scheme 21. IR spectrum of 4a

APPENDIX 3: MS SPECTRA

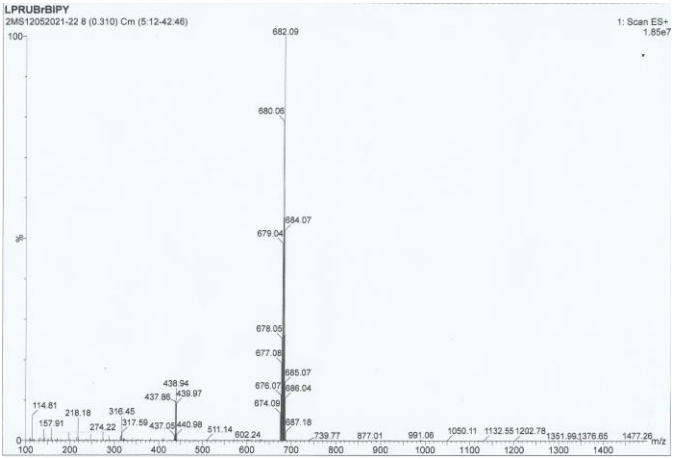

Scheme 22. MS spectrum of **7a**

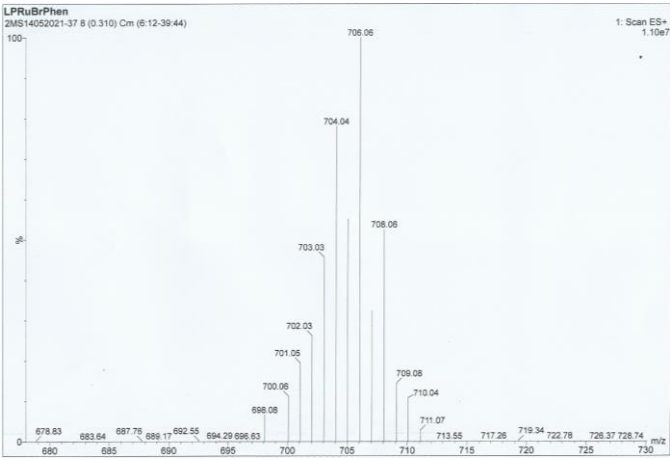

Scheme 23. MS spectra of **7a'**

APPENDIX 4: UV-VIS AND EXCITATION GRAPHICS

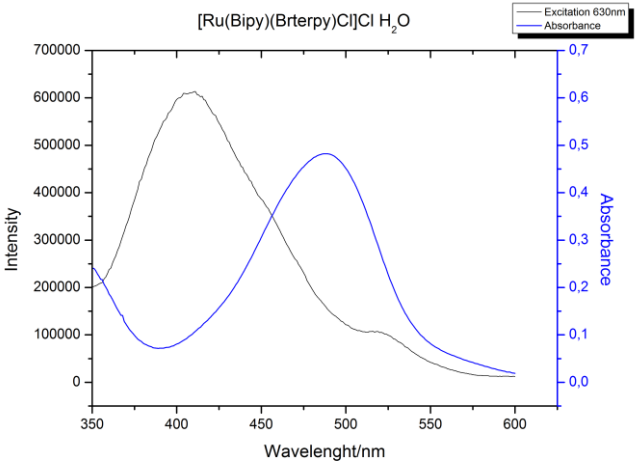

Scheme 24. Absorbance and excitation spectra of **7a** in water

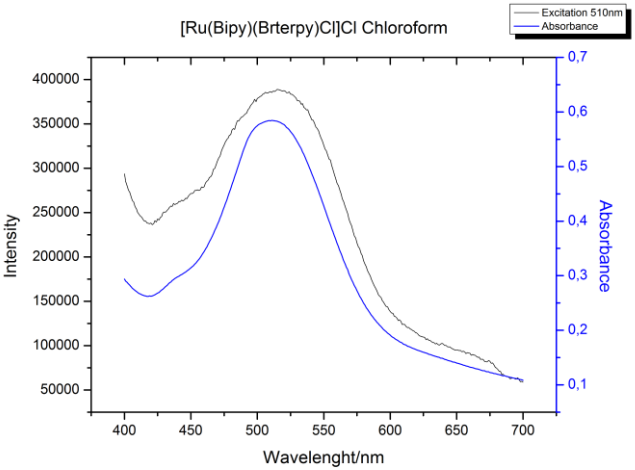

Scheme 25. Absorbance and excitation spectra of **7a** in chloroform

APPENDIX 3: AGAROSE GEL ELECTROPHORESIS IMAGES

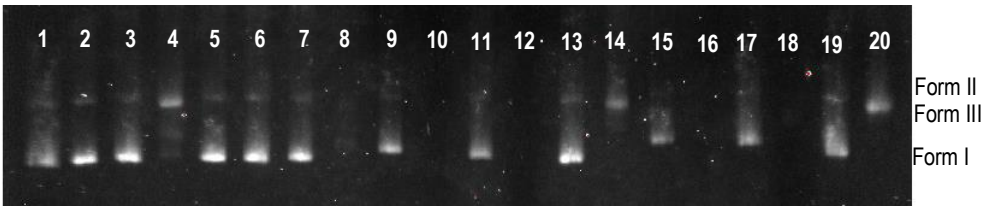

Scheme 26. Agarose gel electrophoresis images of pBR322 plasmid DNA (15 μM b.p.).Lanes 1,2: pure plasmid DNA; lanes 3,4: [$[Ru(Phen)_3]Cl_2$] = 10 μM, lanes 5,6 [**4a**] = 10 μM, lanes 7,8 [**5a**] 10 μM, lanes 9,10 [**7a**] 50 μM, lanes 11,12 [**7a**] 25 μM, lanes 13,14 [**7a**] 10 μM, lanes 15,16 [**7a'**] 50 μM, lanes 17,18 [**7a'**] 25 μM, lanes 19,20 [**7a'**] 10 μM.